

ARTICLE



Modeling *SHANK3*-associated autism spectrum disorder in Beagle dogs via CRISPR/Cas9 gene editing

Rui Tian^{1,8}, Yuan Li^{2,8}, Hui Zhao^{1,3,8}, Wen Lyu¹, Jianping Zhao², Xiaomin Wang³, Heng Lu^{4,5}, Huijuan Xu¹, Wei Ren¹, Qing-quan Tan¹, Qi Shi¹, Guo-dong Wang⁵, Ya-ping Zhang⁵, Liangxue Lai³, Jidong Mi^{2,9}, Yong-hui Jiang^{6,9} and Yong Q. Zhang^{1,7,9}

© The Author(s), under exclusive licence to Springer Nature Limited 2023

Despite intensive studies in modeling neuropsychiatric disorders especially autism spectrum disorder (ASD) in animals, many challenges remain. Genetic mutant mice have contributed substantially to the current understanding of the molecular and neural circuit mechanisms underlying ASD. However, the translational value of ASD mouse models in preclinical studies is limited to certain aspects of the disease due to the apparent differences in brain and behavior between rodents and humans. Non-human primates have been used to model ASD in recent years. However, a low reproduction rate due to a long reproductive cycle and a single birth per pregnancy, and an extremely high cost prohibit a wide use of them in preclinical studies. Canine model is an appealing alternative because of its complex and effective dog–human social interactions. In contrast to non-human primates, dog has comparable drug metabolism as humans and a high reproduction rate. In this study, we aimed to model ASD in experimental dogs by manipulating the *Shank3* gene as *SHANK3* mutations are one of most replicated genetic defects identified from ASD patients. Using CRISPR/Cas9 gene editing, we successfully generated and characterized multiple lines of Beagle *Shank3* (*bShank3*) mutants that have been propagated for a few generations. We developed and validated a battery of behavioral assays that can be used in controlled experimental setting for mutant dogs. *bShank3* mutants exhibited distinct and robust social behavior deficits including social withdrawal and reduced social interactions with humans, and heightened anxiety in different experimental settings ($n = 27$ for wild-type controls and $n = 44$ for mutants). We demonstrate the feasibility of producing a large number of mutant animals in a reasonable time frame. The robust and unique behavioral findings support the validity and value of a canine model to investigate the pathophysiology and develop treatments for ASD and potentially other psychiatric disorders.

Molecular Psychiatry; <https://doi.org/10.1038/s41380-023-02276-9>

INTRODUCTION

Autism spectrum disorder (ASD), affecting roughly 1% of the population worldwide, is a neuropsychiatric condition characterized by social communication and interaction deficits, and repetitive and restricted behaviors or interests. Substantial progress in identifying genetic defects contributing to ASD has provided the construct validity to model ASD in animals [1–5]. Genetically engineered mice that carry mutations identified in ASD patients have contributed substantially to the current understanding of molecular and circuit mechanisms underlying ASD. However, because of the substantial differences in brain, behavior, and drug metabolism between rodents and humans, preclinical studies devoted to the development of new treatments for ASD have raised questions about the translational utility of rodent models for drug development of brain disorders [6, 7]. The efficient genome editing techniques and virus-based gene

manipulations have made it possible to model ASD in species such as non-human primates [8–12]. The non-human primate models provide new insights into the pathophysiology of ASD. However, the low reproduction rate (5 years to reach sexual maturity and one progeny per pregnancy) and the extremely high cost pose a practical challenge for the broad application of these models in preclinical studies [6, 13, 14].

Domestic dogs offer an excellent alternative to explore the feasibility of modeling ASD and other neuropsychiatric diseases. The dog genome more closely resembles the human genome than the mouse genome in sequence composition [15]. The spatiotemporal expression pattern of dog brain proteome is more similar to that of human brain than that of mouse brain [16]. Dogs show stronger social bonds with humans than non-human primates through reading human communicative cues such as pointing and gazing [17–20]. Thus, dogs may have unique

¹State Key Laboratory of Molecular Developmental Biology, and CAS Center for Excellence in Brain Science and Intelligence Technology, Institute of Genetics and Developmental Biology, Chinese Academy of Sciences, Beijing 100101, China. ²Beijing Sinogene Biotechnology Co. Ltd, Beijing, China. ³Key Laboratory of Regenerative Biology, South China Institute for Stem Cell Biology and Regenerative Medicine, Guangzhou Institutes of Biomedicine and Health, Chinese Academy of Sciences, Guangzhou 510530, China. ⁴Department of Life Science and Medicine, University of Science and Technology of China, Hefei 230022, China. ⁵State Key Laboratory of Genetic Resources and Evolution, and Center for Excellence in Animal Evolution and Genetics, Kunming Institute of Zoology, Chinese Academy of Sciences, Kunming 650201, China. ⁶Department of Genetics and Neuroscience, Yale University School of Medicine, New Haven, CT 06510, USA. ⁷Present address: School of Life Sciences, Hubei University, Wuhan, China. ⁸These authors contributed equally: Rui Tian, Yuan Li, Hui Zhao. ⁹These authors jointly supervised this work: Jidong Mi, Yong-hui Jiang, Yong Q. Zhang. ✉email: yong-hui.jiang@yale.edu; yqzhang@genetics.ac.cn

Received: 18 January 2023 Revised: 30 August 2023 Accepted: 14 September 2023

Published online: 17 October 2023

advantages over rodents and non-human primates for studying ASD and other psychiatric disorders, owing to their efficient and readily interpretable social interactions with humans.

We aim to explore the potential of using genetically modified dogs to model neuropsychiatric diseases. Since *SHANK3* mutation is the first and one of the most replicated genetic risks for idiopathic ASD [1–5, 21, 22] and our team has extensive experience in modeling *SHANK3*-associated ASD in mice and monkey [10, 11, 23, 24], we aimed to develop *Shank3* mutant dog models for this exploratory investigation. In the present study, we generated and characterized multiple lines of mutant dogs carrying distinct mutations in Beagle *Shank3* (*bShank3*) by CRISPR/Cas9 gene editing. Among the various breeds of dogs, we chose Beagles as they are considered as an ideal breed for biomedical research and new drug development because of its docility, relatively small size, and similar drug metabolism to humans [25, 26]. Furthermore, for the first time, we developed and validated several behavioral assays to assess ASD-like behaviors in mutant dogs. *bShank3* mutant dogs recapitulate social behavior deficits including social withdrawal and elevated anxiety reported in human ASD patients. To our knowledge, this is the first report of modeling ASD in dogs by a genetic approach. Our findings demonstrate the validity and advantages of genetically modified dogs to model ASD and possibly other psychiatric diseases.

RESULTS

CRISPR/Cas9-mediated gene editing of *bShank3* in Beagle dogs

To generate *bShank3* mutants by CRISPR/Cas9 gene editing, we targeted exon 5 and exon 21 independently to disrupt the ANK domain and proline-rich domain of *bShank3*, respectively, and also exons 5 and 21 simultaneously to induce a large deletion between them (Fig. 1a). From 17 pregnancies of 84 injected zygotes, we obtained 51 F0 offspring, of which 13 carried mutations in *bShank3* (25.5% positive rate for gene editing) as determined by PCR and Sanger sequencing (Supplementary Fig. S1).

Whole-genome sequencing, which allows unbiased detection of sequence variants across the genome, of F0 mutants including Mu216M, Mu306M, Mu614F, and Mu636F showed apparently reduced coverage in targeted sites (Fig. 1b). In support of the whole-genome sequencing results, genotyping analysis by PCR followed by DNA sequencing revealed bi-allelic mutations in exon 21 from Mu216M (–496/–522 bp), Mu306M (–483 + 7/–1279 + 1 bp), and Mu636F (–4/–12 + 1 bp) (Fig. 1b, c and Supplementary Fig. S1). These mutations except –522 bp (resulting in an in-frame deletion of 174 amino acid residues) lead to frame shifts and truncated proteins ending at the proline-rich domain (PRO) (Fig. 1a, b, d). Mu614F carried a large deletion of ~33 kb (–33752 + 16 bp) spanning exons 5 and 21, reducing the sequence coverage by 37.64% calculated from the whole-genome sequencing data, together with a low mutation rate (1/12) of –4 bp in exon 21 (Fig. 1b and Supplementary Fig. S1).

To obtain germline transmission of the mutations from F0 founder mutants, we bred Mu216M and Mu306M with wild-type (WT) females and obtained F1 offspring carrying expected heterozygous *bShank3* mutations. We then crossed these F1 heterozygotes except the ones carrying mutations of –522 bp to generate F2 and F3 mutants for phenotypic analysis. However, we had no success in obtaining viable offspring from F0 female mutants of Mu614F and Mu636F, as they experienced multiple premature deliveries (twice for Mu614F and once for Mu636F), partly due to a low level of progesterone in late pregnancy.

We examined *bShank3* expression in the prefrontal cortex (PFC) of deceased newborn F1 and F2 mutants (postnatal days 1–5) by immunoblot analysis with a rabbit antibody we generated against the C-terminus 1453–1805 aa of mouse *Shank3* [10]. A

substantially reduced level of *bShank3* was observed in heterozygous F1 offspring, and even more so in homozygous F2 mutants (Fig. 1d), consistent with the expected mutations at the protein level (p.G1072PfsX37 for the –496 bp deletion and p.P1071LfsX77 for the –483 + 7 bp indel based on the reference protein sequence XP_038535340.1). An extra band of 190 kD observed in –1279 + 1 bp mutants is likely due to an expected 426 aa in-frame deletion (p.P1063_K1488del; Fig. 1d). These results indicate a deficiency of the majority of *bShank3* isoforms but certain isoforms remaining in these mutants, similar to the findings from different lines of *Shank3* mutant mice with various targeted mutations [21, 27]. CRISPR/Cas9 editing could cause off-target mutations. To test this possibility, we analyzed whole-genome sequencing data of the founder dogs and their parents (the raw sequence data can be accessed at <https://bigd.big.ac.cn/gsa> with accession number CRA004090). These analyses did not reveal any off-target mutations, consistent with previous reports on the fidelity CRISPR/Cas9-mediated mutations in non-human primates [10, 12, 28].

To understand the molecular consequence of *bShank3* mutations, we examined expression levels of neuronal markers NeuN and Doublecortin (DCX), the glutamate receptor GluN2B, and PSD proteins PSD95, Homer, and Homer1b/c in whole-cell lysates of PFC from WT controls and mutants at P0–P5 by western analysis; homozygous –496 bp but not 1279 + 1 bp mutants expressed significantly decreased levels of NeuN, DCX and GluN2B (Fig. 2a, b). Immunohistochemistry analysis verified the western results of decreased NeuN expressions in homozygous –496 bp mutants (Fig. 2c, d). The decreased levels of NeuN, DCX and GluN2B in homozygous –496 bp mutants are consistent with our previous findings in a *SHANK3* mutant monkeys [10].

General health and development of *Shank3* mutants

The offspring of two F0 founder mutants Mu216M and Mu306M including 33 heterozygotes, 3 compound heterozygotes, and 8 homozygotes of F1–F3 offspring were phenotypically analyzed in the present study (Supplementary Table 1). For simplicity, we grouped compound heterozygous and homozygous mutants together as homozygotes (–/–) hereafter, since we did not observe a significant difference between them. A total of 27 WT controls including WT littermates were included in this study. WT littermates ($n = 6$) were used as preferred controls if they were available. Otherwise, age- and gender-matched and typically developed dogs were used as WT controls. Homozygous *bShank3* mutants showed significantly reduced body size and weight (controls: 13.2 ± 2.19 kg (mean \pm SD throughout); homozygotes: 9.91 ± 1.80 kg, $F_{(2,60)} = 9.011$, $p = 0.003$), but all heterozygous *bShank3* mutants (12.51 ± 2.22 kg, $F_{(2,60)} = 9.011$, $p = 0.4788$) were comparable to WT controls in size and body weight (Fig. 2e). We noted that F0 mutants showed compromised locomotion in treadmill assay and stair climbing. However, the F1 and F2 mutants, heterozygous or homozygous, performed normally on the assays, suggesting the locomotion defects in F0 mutants might not be associated with *bShank3* mutations. Consistently, the locomotive activities of F1 and F2 mutants monitored by an accelerometer actigraphy in home cages in both day time and night time appeared normal (Fig. 2f).

Observation of social play in a natural setting has been the major paradigm for behavioral analysis of dogs [19, 29]. Quantitative behavioral assays of genetically modified dogs in controlled experimental setting have thus far not been reported. In order to assess social behaviors of *bShank3* mutant dogs, we developed and performed a battery of behavioral assays including three-chamber analysis, social interaction with human in home cage and in open field (OF), machine learning-assisted analysis of tail wagging, and attention-seeking test of *bShank3* mutants and WT controls. The order for different behavioral assays is presented in Fig. 3a.

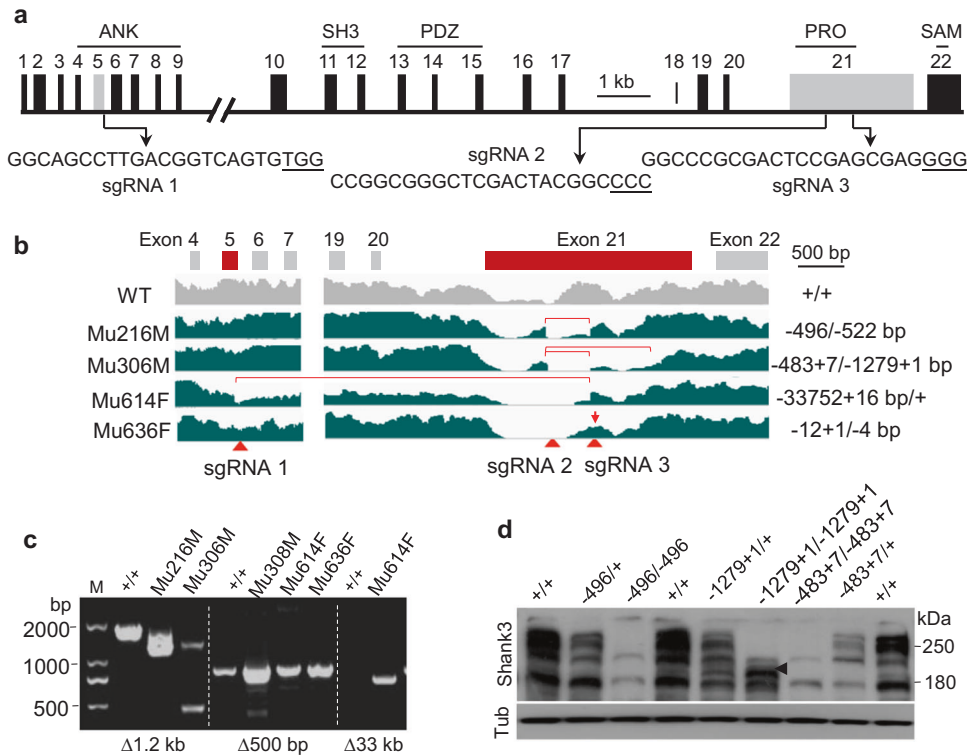


Fig. 1 CRISPR/Cas9-mediated *bShank3* mutations in dogs. **a** Schematic diagram of *bShank3* (genomic DNA MW32209 at Genbank) and sgRNAs targeting sites in exons 5 and 21. The distance between sgRNA1 and 3 is 33 kb, and 440 bp between sgRNAs 2 and 3. **b** Whole-genome sequencing in sgRNA-targeted regions in wild-type (gray) and mutant (cyan) dog genomes. The horizontal red lines highlight the deletions in Mu216M, Mu306M, and Mu614F and the red arrow indicates the small indels identified in Mu636F mutant. More detailed information on these mutants at the DNA level is included in Suppl. Figure 1. The target sites of sgRNA1, 2, and 3 are denoted by red triangle. **c** PCR analysis of F0 founder mutants Mu216M, Mu306M, Mu308M, Mu614F and Mu636F with primers detecting ~1.2 kb and ~500 bp deletions in exon 21, and a large deletion of ~33 kb spanning exon 5 and exon 21. **d** Representative immunoblots of *bShank3* in PFC total lysates probed with an antibody against the C-terminus of mouse Shank3. Black arrow points to an extra band of 190 kDa in the lysate of -1279 + 1/-1279 + 1 bp mutant.

Social interaction deficits with conspecific dogs in *bShank3* mutant dogs

Three-chamber test has been widely used for the investigation of sociability and novelty preference in ASD mouse models including *Shank3* mutant mice [30–32]. To examine social interactions of *bShank3* mutant dogs, we designed a three-chamber test for dogs adapted from the protocol for mice (Fig. 3b and Supplementary movie 1). WT dogs of 4–12 months old displayed sociability and social novelty preference (Fig. 3c), similar to that in mice [30, 31]. Specifically, WT dogs spent more time in the chamber containing stranger 1 (Str1) than the empty cage (social preference) in phase 1, and more time in the chamber containing stranger 2 (Str2) than Str1 (novelty preference) in phase 2 (Fig. 3c and Supplementary table 2). Heterozygous *bShank3* mutants displayed normal social preference, but novelty preference deficit (Fig. 3c). Homozygous *bShank3* mutants displayed both social preference and novelty preference deficits compared with WT dogs (Fig. 3c).

However, we observed apparent social withdrawal behaviors in *bShank3* mutants in the three-chamber test. We defined social withdrawal as a dog approached, i.e. moved towards or engaged a stranger dog in the side-chamber, but then retreated, looked away, or became inactive. *bShank3* mutants showed a normal frequency of social approaches, but exhibited a higher percentage of social withdrawal immediately after approaching a stranger dog compared to WT controls (controls: $0.40 \pm 1.24\%$; heterozygotes: $5.367 \pm 8.19\%$, $p = 0.004$; homozygotes: $2.52 \pm 3.61\%$, $p = 0.1451$; Fig. 3d and Supplementary Table 2).

During the three-chamber assay, we observed a difference in tail wagging between mutants and WT controls. Posture and

movement of dog tails are considered as a real-time indicator of inner emotional state during conspecific and dog–human communications [33–36]. The tail is held high to communicate confidence, arousal, or willingness to approach another individual during greeting and playing, but held stiff and low or tucked between hind limbs indicating anxiety and fear [35, 37], for which we named them collectively as negative tails. Both heterozygous and homozygous *bShank3* mutants displayed a significantly longer duration (control: 29.50 ± 118.3 s; heterozygotes: 334.1 ± 359.0 s, $p < 0.0001$; homozygotes: 243.6 ± 339.0 s, $p = 0.0076$) and a higher frequency of negative tails than WT dogs (controls: 0.550 ± 1.669 times; heterozygotes: 5.214 ± 5.884 times, $p = 0.0001$; homozygotes: 4.364 ± 4.433 times, $p = 0.0039$); few WT dogs exhibited negative tails during the three-chamber test (Fig. 3e and Supplementary movie 1 and table 2).

Impaired social interaction with humans in *bShank3* mutants

One unique advantage of the dog model for ASD study is that dogs possess an exceptional capability of carrying out complex and exquisite social interactions with humans [17–19, 38]. To examine social interaction of *bShank3* mutants with humans, we designed dog–human interaction assays with dogs in the home cage and in an open field (OF) (Fig. 4a, b). When in the home cage, WT dogs showed a great interest in the familiar person, i.e., following, sniffing or licking the person. However, *bShank3* mutant dogs showed less interest in the experimenter, i.e., significantly reduced duration (controls, 24.62 ± 6.50 s; heterozygotes, 15.30 ± 11.13 s, $p = 0.0074$; homozygotes, 9.40 ± 8.14 s, $p = 0.0004$) and frequency (controls, 3.60 ± 0.77 times/30 s;

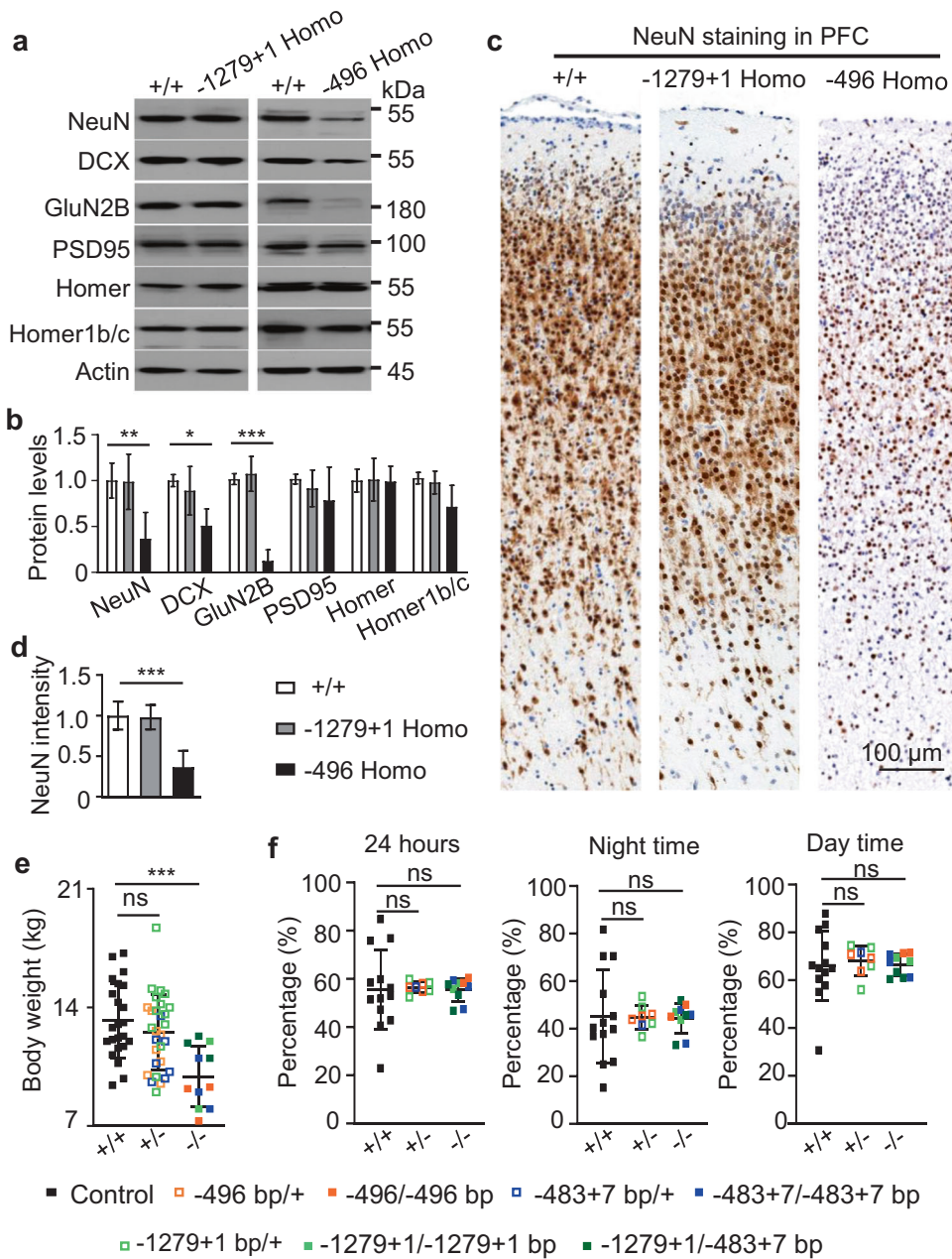


Fig. 2 Reduced neuronal markers and GluN2B in *bShank3* mutant brains. **a** Western blot analysis of neuronal markers NeuN and DCX, glutamate receptor GluN2B, and PSD proteins PSD95, Homer and Homer1b/c in whole-cell lysates of PFC from WT controls and *bShank3* mutants at P0–P5. Homozygous -496 bp mutants expressed decreased levels of NeuN, DCX, and GluN2B. **b** Statistical analysis of western results shown in (a). Western analysis was repeated biologically at least three times. * $p < 0.05$, ** $p < 0.01$, and *** $p < 0.001$ by one-way ANOVA. **c** NeuN staining validated a reduced level of NeuN in homozygous -496 bp but not -1279 + 1 bp mutant PFC. **d** Statistical analysis of NeuN staining intensities. Three images from each animal of 0.2 mm² area in layer 2 to layer 6 of PFC was quantified. *** $p < 0.001$ by one-way ANOVA. $N = 3$ animals for +/+, $n = 2$ and 3 for homozygous -1279 + 1 bp and -496 bp mutants, respectively. **e** Adult body weights of controls and heterozygous and homozygous *bShank3* mutants. Genotypes are indicated by colored boxes and blocks. +/+, WT controls; +/-, combined heterozygotes of -496 bp/+, -483 + 7 bp/+, and -1279 + 1 bp; -/-, combined compound heterozygotes (-1279 + 1/-483 + 7 bp) and homozygotes (-496/-496 bp, -483 + 7/-483 + 7 bp, and -1279 + 1/-1279 + 1 bp). $N = 23$, 29, and 11 for WT controls, heterozygotes, and homozygotes, respectively. **f** Normal locomotor activities including 24 h activity, day time and night time activity in heterozygous and homozygous *bShank3* mutants. $N = 13$, 8, and 10 for WT controls, heterozygotes, and homozygotes, respectively. Data are presented as mean \pm SD. * $p < 0.05$; ** $p < 0.01$; *** $p < 0.001$ by one-way ANOVA.

heterozygotes, 2.42 ± 1.47 times/30 s, $p = 0.0053$; homozygotes, 2.10 ± 1.37 times/30 s, $p = 0.0088$) of human following when the experimenter walked back and forth in front of the cage in the step 1 of the test (Fig. 4c and Supplementary table 3). When the experimenter moved his/her hands on the cage in the step 2 of the test, *bShank3* mutants showed significantly fewer sniffs or licks of the experimenter's fingers compared with control dogs;

the duration of sniffs or licks was 8.14 ± 5.86 s and 2.90 ± 4.01 s for heterozygous and homozygous mutants, respectively, significantly shorter than 13.10 ± 6.40 s of the controls; so was the frequency of sniffs or licks in *bShank3* mutants (Fig. 4d and Supplementary Table 3). More negative tails were also consistently observed in *bShank3* mutants during dog–human interactions (Fig. 4e).

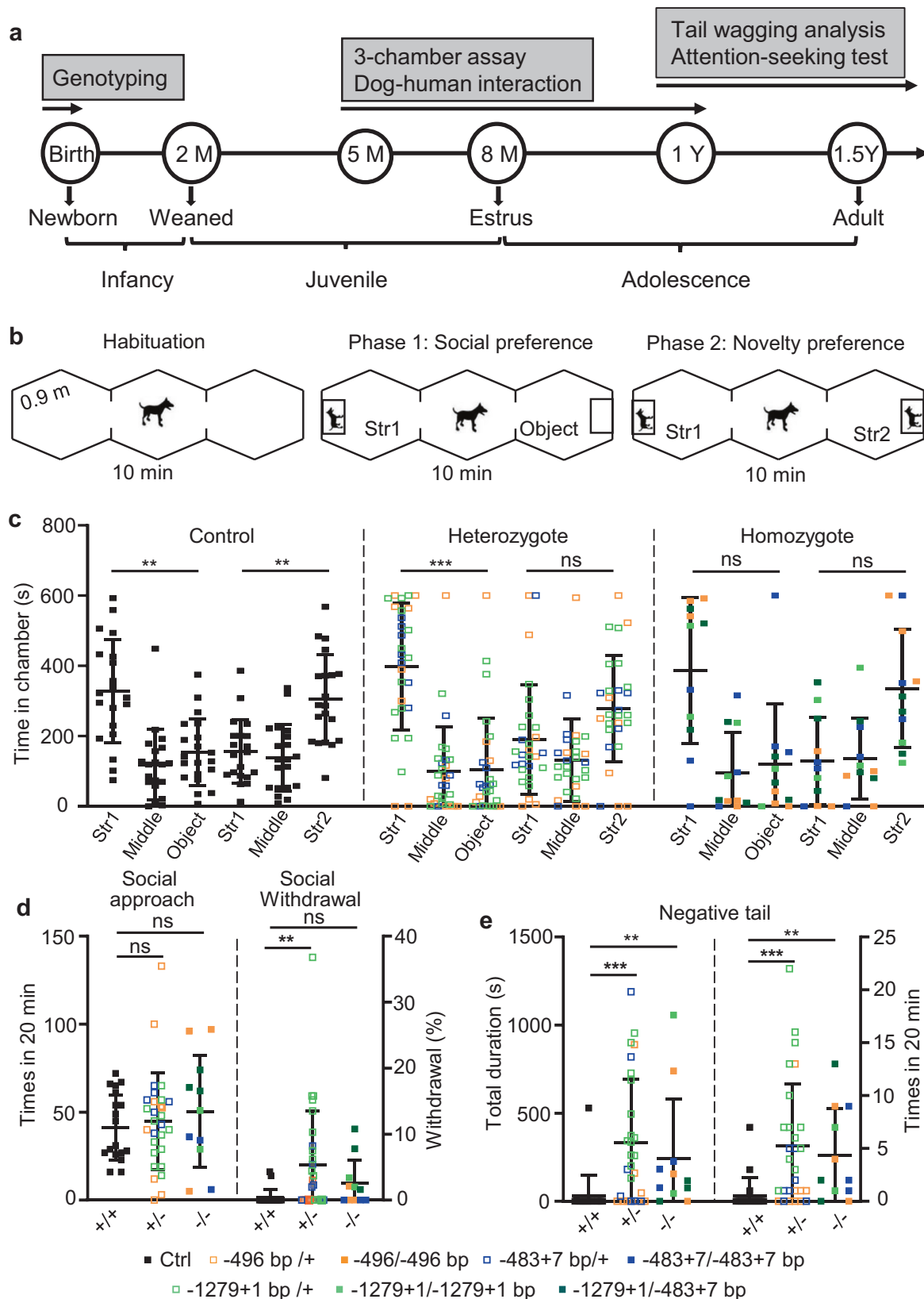


Fig. 3 *bShank3* mutants show impaired social interaction and increased social withdrawal in three-chamber test. **a** The timeline of behavioral assays. **b** The diagram of dog three-chamber test for sociability and social novelty preference. **c** Time spent in each chamber of *bShank3* mutants and controls during sociability (phase 1) and novelty preference test (phase 2). *bShank3* mutant dogs showed increased social withdrawal (**d**), and increased duration and frequency of negative tails (**e**) in the three-chamber test. Each square indicates the value of each animal for the first trial of the assay. Data are presented as mean \pm SD. $N = 20, 28,$ and 11 for WT controls, heterozygotes, and homozygotes, respectively. * $p < 0.05$; ** $p < 0.01$; *** $p < 0.001$ by one-way ANOVA.

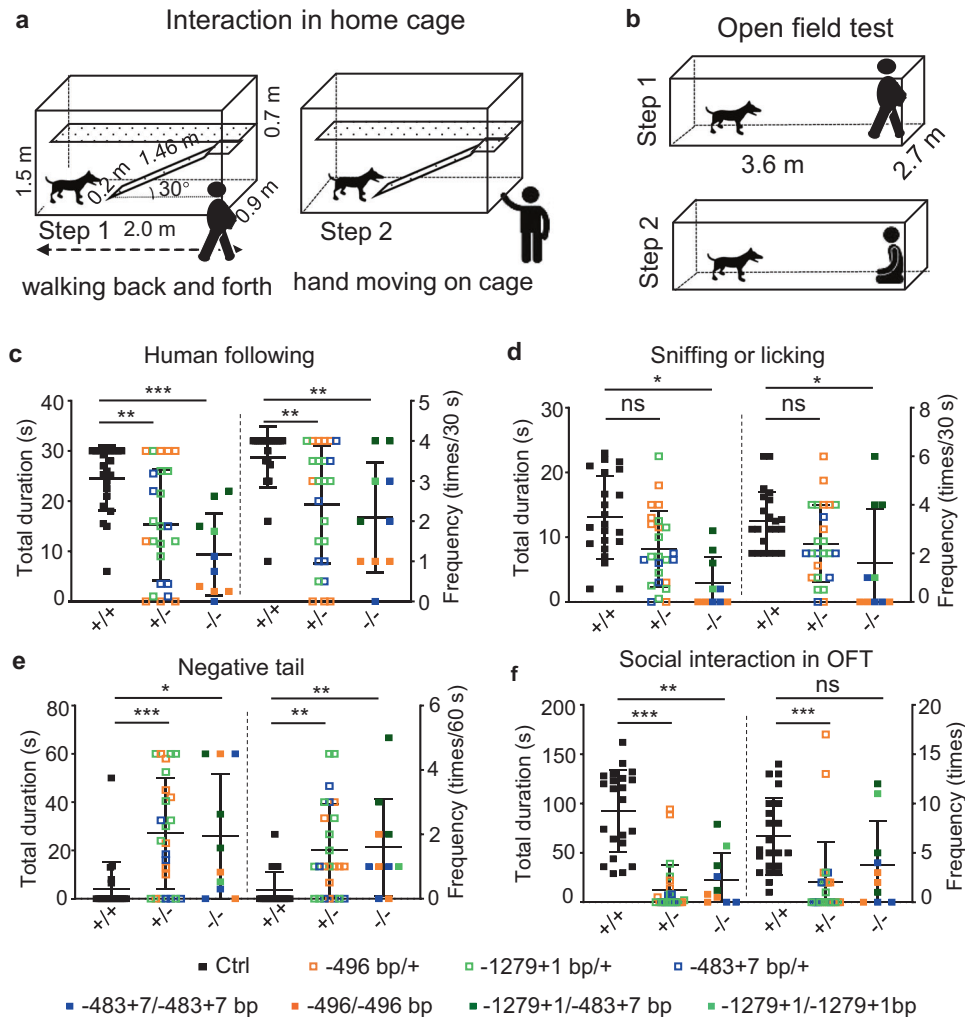


Fig. 4 Deficits of social interaction with human in *bShank3* mutants. Schematic diagram of dog–human social interaction assay in the home cage (a) and an open field (b). *bShank3* mutants showed significantly reduced duration and frequency of human-following behavior in step 1 (c) and sniffing/licking in step 2 (d). **e** *bShank3* mutants exhibited significantly longer duration and higher frequency of negative tails when interacting with humans in home cage. **f** *bShank3* mutants showed significantly decreased duration and frequency of social interactions with humans in open field. Each square represents the value of each animal for the first trial of the assay. Data are presented as mean \pm SD. $N = 22$, 25, and 10 for WT controls, heterozygotes, and homozygotes, respectively. * $p < 0.05$; ** $p < 0.01$; *** $p < 0.001$ by one-way ANOVA.

In the OF test, control dogs showed more intimate interactions, i.e., more body contacts such as rearing and climbing on the familiar person while *bShank3* mutants appeared to be submissive and cowering (Supplementary Movie 2). Consistent with the results of reduced social interactions in home-caged mutants, we also observed significantly reduced duration (controls, 92.40 ± 41.53 s; heterozygotes, 12.56 ± 25.74 s, $p < 0.0001$; homozygotes, 22.40 ± 27.39 s, $p = 0.0017$) and frequency (controls, 6.71 ± 3.90 times/240 s; heterozygotes, 2.00 ± 4.11 , $p < 0.0001$; homozygotes, 3.80 ± 4.42 times/240 s, $p = 0.0714$) of social interactions including rearing, gazing, following, licking or sniffing the experimenter in *bShank3* mutants in the OF test (Fig. 4f and Supplementary Movie 2 and Table 4). The homozygous -496 bp mutants appeared to have a stronger deficit in dog–human interactions than the other mutants. However, the difference did not reach significance in all four parameters (Fig. 3c–f), probably due to a small number of animals tested. These results together show that *bShank3* mutants exhibit significantly impaired social interactions with humans.

During the dog–human interactions, we consistently observed apparently reduced tail wagging in *bShank3* mutants. To quantify the kinematics of tail wagging during the heterospecific interactions, we previously developed a protocol using a machine

learning-based motion-tracking technique to extract and analyze the movement trajectory of a dog's tail tip [36]. Using the technique (Fig. 5a, b and Supplementary Movie 3), we quantitatively analyzed the three kinematic parameters of tail wagging: the frequency (the number of wagging bouts in a second; a wagging bout is defined as a segment of wagging from the most-left to the most-right side and back again), amplitude (absolute difference in adjacent angles of tail wagging, ranging from 0° to 360°), and velocity (angular velocity of wagging, ranging from $0^\circ/\text{frame}$ to $16^\circ/\text{frame}$) of tail wagging. *bShank3* mutant dogs showed significantly decreased tail wagging, i.e., reduced frequency (controls, 2.90 ± 0.16 bouts/s; heterozygotes, 1.92 ± 0.98 bouts/s, $p = 0.008$; homozygotes, 2.05 ± 0.67 bouts/s, $p = 0.0057$), amplitude (controls, $97.23 \pm 31.83^\circ$; heterozygotes, $44.40 \pm 34.64^\circ$, $p = 0.0047$; homozygotes, $37.78 \pm 16.17^\circ$, $p = 0.0008$), and velocity (controls, $4.16 \pm 1.24^\circ/\text{frame}$; heterozygous, $1.84 \pm 1.68^\circ/\text{frame}$, $p = 0.0071$; homozygotes, $1.40 \pm 0.81^\circ/\text{frame}$, $p = 0.0011$) compared with WT controls (Fig. 5c–e and Supplementary Table 5).

Elevated anxiety in *bShank3* mutant dogs

The higher occurrence of social withdrawal, stiff and lowered or tucked tails, and greatly reduced tail wagging in *bShank3* mutants

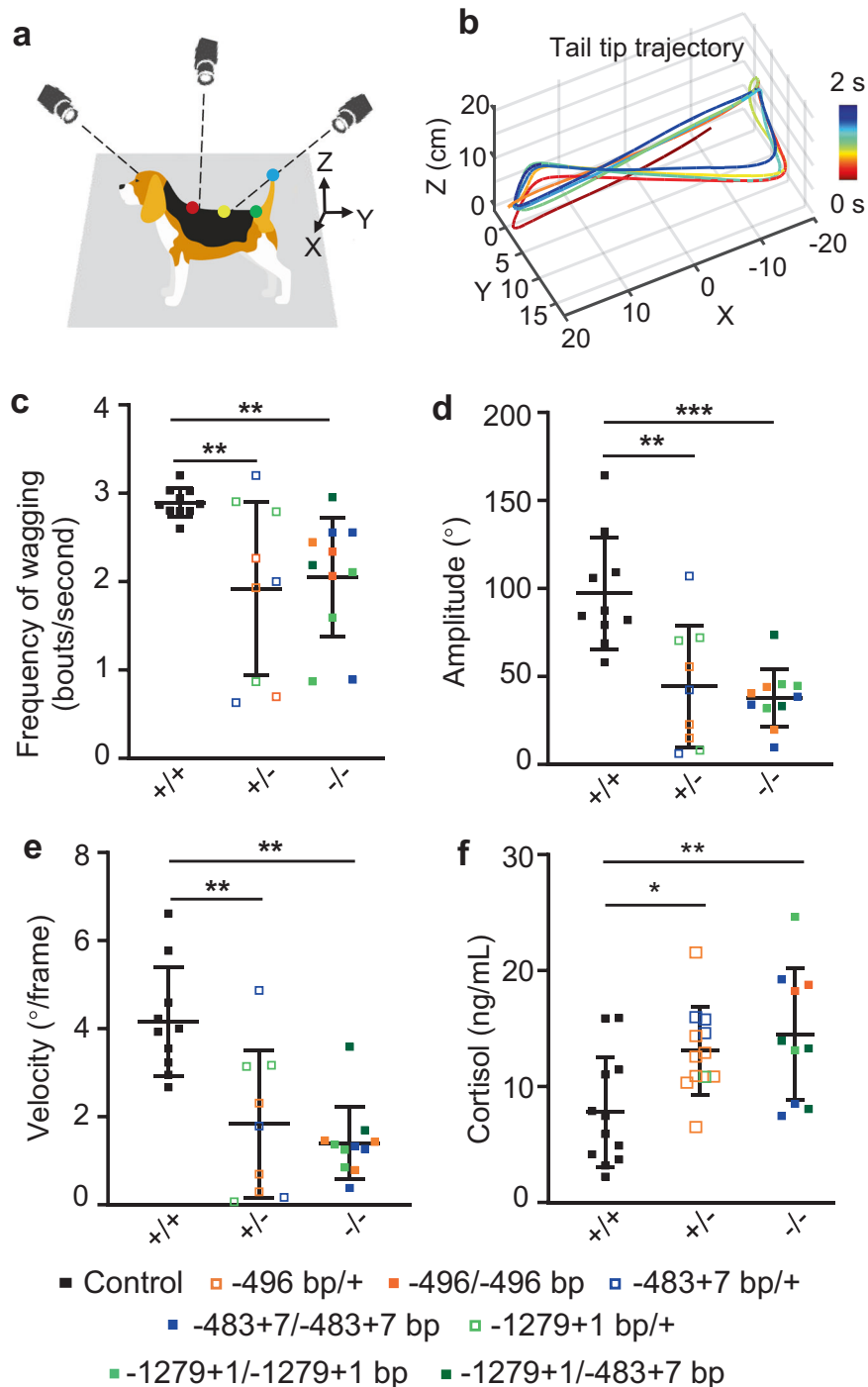


Fig. 5 Reduced tail wagging accompanied by increased blood cortisol in *bShank3* mutants. **a** Diagrams of machine learning-based tracking of wagging tails. **b** A 3D trajectory of a wagging tail tip in 2 s. *bShank3* mutant dogs showed significantly decreased frequency (**c**), amplitude (**d**), and velocity of tail wagging (**e**) during dog–human interaction. $N = 10, 9,$ and 11 for WT controls, heterozygotes, and homozygotes, respectively. **f** *bShank3* mutant dogs showed a significantly increased level of cortisol compared with the wide-type controls. $N = 12, 12,$ and 10 for WT controls, heterozygotes, and homozygotes, respectively. Data are presented as mean \pm SD. * $p < 0.05$; ** $p < 0.01$; *** $p < 0.001$ by one-way ANOVA.

shown above indicate that they may be in a state of heightened stress. To further support this possibility, we measured the blood level of cortisol by radioimmunoassay. Cortisol is considered a major indicator of physiological states in response to stress in most mammals including dogs [39]. Indeed, cortisol is a well-established indicator of enduring stress in dogs [40]. As expected, *bShank3* mutant dogs showed a significantly increased level of blood cortisol (heterozygotes: 13.11 ± 3.78 pg/ml, $F_{(2,31)} = 6.36$, $p = 0.019$;

homozygotes: 14.52 ± 5.65 pg/ml, $F_{(2,31)} = 6.36$, $p = 0.0045$) in comparison with WT controls (7.81 ± 4.76 pg/ml) (Fig. 5e), indicating a significantly higher level of anxiety in the mutants.

Delayed soliciting behavior in *bShank3* mutant dogs

Through domestication, dogs, but not their ancestor wolves, have developed ability to seek attention from human during a task of problem solving [18, 41]. To examine the attention-seeking ability

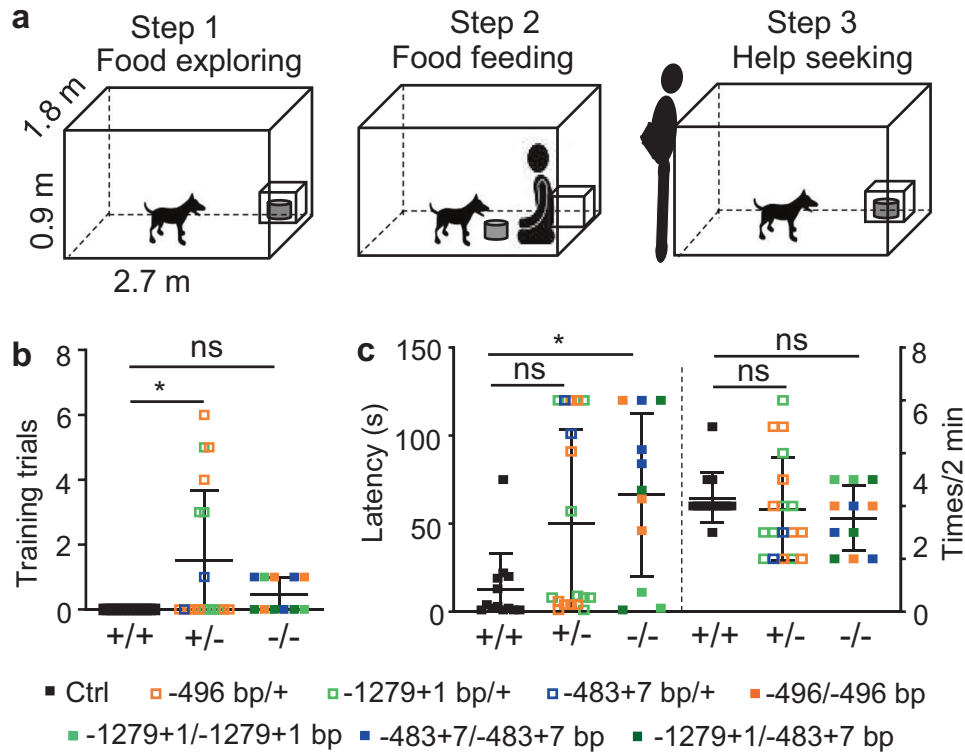


Fig. 6 Delayed attention-seeking behavior in *bShank3* mutants. **a** A diagram of three-step attention-seeking assay. **b** More training trials of getting food from the experimenter were needed for *bShank3* mutants to start the step 1. **c** Longer latency of attention-seeking (looking/gazing at the experimenter) in *bShank3* mutants in step 3 test (left panel). No significant difference in attention-seeking frequency between controls and mutants (right panel). Each data point indicates the value of each animal for the first trial of the test. Data are presented as mean \pm SD. $N = 13, 18,$ and 11 for WT controls, heterozygotes, and homozygotes, respectively, for **b** and **c** panels. * $p < 0.05$; ** $p < 0.01$; *** $p < 0.001$ by one-way ANOVA.

of *bShank3* mutants, we developed a three-step experiment based on a previous report [41] (Fig. 6a and Supplementary movie 4). In the experiment, dogs were exposed to their favorite food of canned chicken, but could not get the food locked in a cage by themselves without the help from the experimenters. In step 1 of familiarization phase of the test (Fig. 6a), controls and mutants showed no difference in exploring the food-containing cage in the absence of an experimenter. In step 2 of feeding phase, the experimenter opened the cage and fed the dog with a piece of sausage from the cage. In step 3 of the test, the remaining sausage was locked in the cage which cannot be unlocked by the dog. The experimenter stood outside of the fence to observe the dog for 2 min (Fig. 6a). The soliciting behavior was defined as looking back or gazing at the experimenter in the step 3 test.

To qualify for the test of attention-seeking, food-restricted dogs needed to be interested in their favorite sausage hand-presented by the experimenter who were familiar to the dogs. WT dogs were interested in the food at the first time presented by the experimenter. However, mutants appeared to be stressful or fearful with the experiment. It took more trials for *bShank3* mutants to get familiar with the experimenter to get hand-presented food than WT controls (0 trials for controls; 1.50 ± 2.18 for heterozygotes, $p = 0.0208$; 0.36 ± 0.50 for homozygotes, $p = 0.1834$; Fig. 6b and Supplementary Table 6). For the attention-seeking behaviors, *bShank3* mutant dogs showed an increased latency (controls, 12.62 ± 20.43 s; heterozygotes, 50.11 ± 53.63 s, $p = 0.0639$; homozygotes, 66.27 ± 46.37 s, $p = 0.0194$) but a normal number (controls, 2.31 ± 0.95 times/2 min; heterozygotes, 1.89 ± 1.94 times/2 min, $p = 0.2736$; homozygotes, 1.55 ± 1.21 times/2 min, $p = 0.3625$) of the behaviors within the 2 min test compared with the WT controls (Fig. 6c and Supplementary Table 6).

DISCUSSION

In the present a study, we report the first ASD-related mutants created by the CRISPR/Cas9 gene editing technique in dogs. We further characterized these mutants by a battery of behavioral assays which we developed and validated to assess behavioral features of *bShank3* mutant dogs. Our findings demonstrated that disruption of *bShank3* leads to impaired conspecific and hetero-specific social interactions, together with increased anxiety and fear, in several different assays. These social behavior abnormalities represented by social withdrawal in the three-chamber test and reduced dog-human interactions recapitulate the key feature of social behavior deficits associated with ASD. The present study lays an important framework for using genetically modified dogs to model ASD for mechanistic studies as well as preclinical studies for therapeutics development.

Heterozygous *bShank3* dogs showed robust social behavior phenotypes as homozygous mutants when interacting with dogs or humans. The impaired social interaction phenotypes in *bShank3* heterozygotes is consistent with haploinsufficiency of *SHANK3* associated ASD in humans [21, 42–44]. This is in contrast to that only a few lines of *Shank3* mutant mice targeting different domains display abnormal social behavior and increased self-grooming behavior [45–48]. The majority of heterozygous *Shank3* mutant mouse lines have either mild [24] or no apparent behavioral phenotype [21, 32, 49, 50]. For non-human primates, phenotypic analysis has been accomplished thus far only in F0 mosaic *SHANK3* mutant monkeys [10–12].

bShank3 mutant dogs showed normal social approach suggesting sufficient social motivation but did not pursue normal social interaction subsequently in the three-chamber test. Instead, a subset of *bShank3* mutants displayed withdrawal behaviors immediately after social approach. The social withdrawal in

bShank3 mutant dogs, but not observed so far in autism-associated mutant rodents and monkeys, may be due to failure in reading social cues, execution of social interaction, or both. Alternatively, it might be caused by sensory abnormalities which await to be systematically characterized. Interestingly, a similar feature of social withdrawal has been observed in ASD patients by clinicians or reported by parents [48, 49].

Modeling behavioral features of human ASD in animal models such as rodents has been challenging. Some of these might be related to intrinsic limitation of rodent behaviors due to the evolutionary constraint. For example, more than 70% ASD patients have various comorbidities including anxiety that is observed in 42–56% ASD patients [49, 50]. The altered inner emotional state such as anxiety in ASD patients may not be faithfully recapitulated and statistically quantified in rodent or even non-human primate models. However, the inner emotional state of dogs can be readily recognized and quantitatively analyzed via the posture and movement of tails [35, 36]. *bShank3* mutant dogs showed significantly more occurrence of stiff and lowered or tucked tails together with elevated cortisol than WT controls indicating heightened anxiety. Anxiety may contribute, at least partially, to the social interaction deficits in *bShank3* mutants. It would be interesting to examine if anti-anxiety drugs may ameliorate the anxiety and social behavior deficits in *bShank3* mutants. In addition to heightened anxiety, *bShank3* mutant dogs showed complex social abnormalities including submission and covering during dog–human interactions. The submissive behaviors in *bShank3* mutant dogs may reflect social anxiety. In addition, the lack of social reward, which is more in line with human ASD behaviors, could also be considered. Because of the strong molecular validity of *SHANK3* mutations in ASD patients, we believe that the *bShank3* mutant dogs are a valuable alternative model for ASD. As this study represents the first effort of modeling ASD in dogs using CRISPR/Cas9 technology, more studies to understand the mechanisms underlying the various social behavior deficits and the relevance of these abnormalities to the clinical manifestations of ASD patients are warranted.

Social behaviors are sensitive to intrinsic and extrinsic signals. Though we took great effort to maintain and test individual animals in the same conditions, the social behaviors of each animal of both WT controls and mutants varied to a great extent. Different genetic background could contribute to the individual variability, as the Beagle dogs we used and indeed any domestic dogs are not a pure inbreed. Due to the individual variability and manual scoring of a limited number of mutants carrying a specific mutation, we were neither able to observe a gender effect on social behaviors, nor able to clearly demonstrate gene dose effect and definitely correlate phenotypes with genotypes. Machine learning-based analysis of behaviors, developed and increasingly applied in the last decade [36, 51–55], would be effective to quantify specific social behavioral modules among different individuals in different genotypes with more precision and a higher efficiency than the manual approach. The individual variability in dog models parallels the heterogeneity of distinct clinical manifestations of ASD patients with similar or even identical mutations in the same gene [43, 44]. Despite the individual behavioral variability from specific assays, all the mutants we examined by different assays together showed robust and replicated social interaction deficits, reduced tail wagging, and elevated anxiety characterized by more negative tails and increased blood cortisol.

In summary, we successfully generated and characterized *bShank3* mutant dogs using CRISPR/cas9 editing technique. In the process of characterizing the social defects, we have also characterized the *bShank3* mutants with more specific paradigms such as sensory tests by pupillometry and revealed altered pupil responses to social and non-social stimuli in *bShank3* mutants [56]. Together, *bShank3* mutant dogs exhibited robust anxiety and social interaction deficits that recapitulate the common behavioral

features associated with *SHANK3* mutations in humans. Together, *bShank3* mutant dogs exhibited key behavioral features of *SHANK3*-associated ASD in humans. Compared with rodent and non-human primate models, the dog mutant model we developed in the present study shows a unique feature of cross-species dog–human social interactions that offers an ideal opportunity to better recapitulate the distinct social behavior impairments in ASD patients. In addition, the ability to propagate a large number of mutant animals in a short period of time (8–12 months to reach sexual maturity, three pregnancies in two years and 4–6 progeny per pregnancy) at a relatively low cost renders dogs a practically feasible model for studying diseases including ASD. We envision that the value of using dogs to model ASD and common comorbidities such as heightened anxiety, and perhaps other psychiatric diseases will be increasingly appreciated and fulfilled to elucidate the pathophysiology of ASD and address the urgent need of ASD patients and their families.

MATERIALS AND METHODS

Animal husbandry

All animal-related protocols were approved by the Institutional Animal Care Committee of the Institute of Genetics and Developmental Biology, Chinese Academy of Sciences (AP2019037), and strictly carried out in accordance with the institutional policies for the Care and Use of Laboratory Animals. All animals were housed in pairs in 2 × 0.9 × 1.5 m (length × width × height) cages and maintained on a 12 h/12 h dark light cycle. The humidity was 40–60% and the temperature was between 22 °C and 24 °C. Dogs were fed Royal Canine Chow (Royal pet food company limited, France) twice daily during 8:00–10:00 a.m. and 15:30–17:00 p.m. Water was available from an automatic watering device. Based on the veterinary assessment, all dogs were in good health at the time of various experiments and tests. Animals were raised in pairs after weaning at postnatal day 50 and played with caregivers or experimenters for half an hour every week after weaning until 6 months old. All behavioral tests were performed at similar time of the day (9:00–12:00 or 14:30–17:00). The life experience of each animal was kept as similar as possible to minimize individual variability. Female dogs were not in estrus during behavioral analysis. Animals of each group were randomly selected and tested.

Generation of *Shank3* mutant dogs by Cas9/sgRNA editing

To generate *bShank3* mutants, we used a Cas9/sgRNA-based protocol that we described in a previous report [57]. Estrus staging, zygotes collection, cytoplasmic injection, embryo transfer and pregnancy diagnosis were carried out following our previous report [57]. Three effective sgRNAs validated in the primary fibroblast cells of dogs were microinjected into the pronuclear-stage embryos. hSpCas9 plasmid was obtained from Addgene (#42230). T7 promoter was used for in vitro transcription of *Cas9* mRNA and sgRNA. One-cell embryos were collected at 18–24 h after natural mating. Each zygote was injected with 1–5 μ l mixture of *Cas9* mRNA (200 ng/ μ l) and sgRNAs (25 ng/ μ l each). The pregnancy was diagnosed by ultrasonography at 25 days after embryo transfer. All live puppies were kept with their own mothers before natural weaning.

Genotype analysis of targeted sites

All potential mutants and their offspring were genotyped for *bShank3* mutations with DNA extracted from ear and tail collected within one week after birth. Primers used to examine mutations in intron/exon 5 were GACTCAGGAGGTGAGAAGCAGAG and ACATGCGTGCGGACACAT ATAGTC (759 bp product from WT sample). Primer pairs CCTTCAGCGCCAGCATCTTC and GAGCGTGTGCTTTGTTTCAG CTG (1729 bp), and CCTTCAGCGCCAGCATCTTC and TGCAGAGACGTGTCCAGGAC (811 bp) were used to examine indels in exon 21. Primer pairs GACTCAGGAGGTGAGAAGCAGAG and CCCTGGTCTCTCATCTACTGG (34403 bp) were used to detect a large deletion spanning exon 5 and exon 21. The PCR products were directly sequenced or sub-cloned and subsequently sequenced if the PCR products were not homogenous at the DNA level.

On- and off-target analysis by whole-genome sequencing

Whole-genome sequencing was used to analyze on- and off-target CRISPR/Cas9 editing as previously described [58]. Eleven individuals

including eight viable F0 mutants (Mu203F, Mu216M, Mu306M, Mu308M, Mu310M, Mu614F, Mu616F, and Mu636F) and three parents including mother of Mu614F and Mu616F, father of Mu614F, and father of Mu616F were whole-genome sequenced at >30x depth of genome coverage per animal. The sequencing data were mapped to the dog reference genome by BWA-MEM (version 0.7.15) with default parameters, sorted by samtools (version 1.9) [59] and processed (deduplication, indexing) by the Picard Tools (version 1.96) (<http://broadinstitute.github.io/picard/>). IGV (version 2.6.0) were used to visualize the read depth across the *bShank3* gene [60].

Possible off-target sites of sgRNA guided Cas9 endonucleases for *bShank3* with no more than five mismatches were identified using a bioinformatics search tool Cas-OFFinder. All potential off-target sites with homology to the 20-bp sequences (sgRNA plus PAM sequences) were retrieved from the dog reference genome CanFam3.1 [15]. As a result, a total of 5196 possible off-target sites with NAG or NGG PAM sequences were identified. Vcftools (version 0.1.13, <https://vcftools.github.io/index.html>) was used to extract mutations from the gene-edited dataset in the 5196 possible off-target regions.

Western blotting and immunostaining

For western analysis, prefrontal cortex (PFC) was homogenized in RIPA buffer (Hua Xing Bo Chuang, with $1 \times$ protease inhibitor cocktail Set 1 from Sigma) on ice. Protein lysates were separated by SDS-PAGE and transferred onto PVDF membranes (Millipore). The primary antibodies against NeuN (ab104224, Abcam), Doublecortin (4604, Cell Signaling), GluN2B (4212s, Cell Signaling), PSD95 (CP35, Calbiochem), Homer (sc-17842, Santa Cruz), Homer1b/c (sc-20807, Santa Cruz), Actin (MAB1501, Merck Millipore), Tubulin (T5168, Sigma-Aldrich), and mouse Shank3 raised in rabbit were used [10]. The antigen for Shank3 antibody is the C-terminal 1453–1805 aa of mouse Shank3 (NP_067398). α -tubulin was used as a loading control. Immunostaining of PFC with anti-NeuN was performed as previously described [10].

Blood cortisol measurement

Blood samples were collected between 09:00 and 11:00 from the cephalic vein of the dog. Whole blood was drawn into medical vacuum blood collection tube (Sanli, Liuyang, China). The blood samples were centrifuged at $1600 \times g$ for 15 min at 4°C . The serum was collected in a plastic tube and stored at -80°C until assay. Radioimmunoassay for cortisol was detected by the Beijing North Institute of Biotechnology using an Iodine [^{125}I] Cortisol Radioimmunoassay Kit (Beijing North Institute of Biotechnology Co., Ltd, Beijing, China) following the protocol provided by the manufacturer. The minimum level of detection of cortisol was 0.313 ng/ml. The intra- and inter-assay coefficients of variation were <10% and <15%, respectively.

Locomotor activity monitoring

Locomotor activity was recorded in dogs aged 12–24 months for five days in singly housed condition with a wireless accelerometer actigraphy (Motion Watch 8; CamNtech Ltd., Cambridge, UK) which was small ($3.2 \times 3.2 \times 1.1$ cm) and lightweight (18.31 g). The locomotion activity signals were analyzed with Matlab 2019a (MathWorks, USA).

Three-chamber social test

To examine the social interaction between dogs of 4–12 months old, we designed a three-chamber test for dogs based on the classical test for mice [30, 31]. Each chamber is a hexagon puppy pen of 0.9 m for each side. Before test, a dog was allowed to familiarize the chambers and environment freely for 10 min. Then, a stranger dog (stranger 1) in a small cage was placed in one side-chamber, while another empty cage (object) was placed on the other side. The test dog was allowed to move across the three-chambers freely for 10 min; this phase 1 test of social preference could determine if the test dog preferred to play with stranger 1 or object. In phase 2 test of novelty preference, the stranger 2 was then placed in the empty cage and the test dog was again allowed to freely choose to play with stranger 2 or stranger 1 for 10 min. All stranger dogs were the same age and gender as the test dog, and previously habituated to the apparatus for 10 min during the previous day. The chambers were wiped with 70% ethanol and air-dried between tests. The duration and frequency of specific behaviors such as social withdrawal and negative tail during the first trial of the test were analyzed manually by trained experimenters who were blind to the genotype.

Social interaction with humans in home cage and open field

The test of social interaction between home-caged dog and human included two steps: (1) step 1, the experimenter who were familiar to the test dogs walked back and forth twice in front of the home cage for 30 s; (2) step 2, the experimenter placed hands on the cage and moved fingers for 30 s. The duration and frequency of each specific behaviors including human following in step 1, sniffing or licking the experimenter's hands in step 2, as well as negative tails in the first trial of the test were statistically analyzed.

The open field test for dog–human interaction was carried out in a puppy pen of $5.4 \times 4.5 \times 0.9$ m (length \times width \times height) in the morning (9–11 h). The dogs were individually habituated in the puppy pen for 5 min before the test. The dog was then allowed to interact freely for 4 min with the experimenter who was familiar to the test dogs. All behaviors of the dog during the whole test were recorded by a video camera operated by an assistant. The duration and frequency of social interactions with the experimenter in the first trial of the assay were statistically analyzed.

Attention-seeking behavior assay

The attention-seeking behavior assay was developed based on previous reports [18, 41] and carried out in a puppy pen of $2.7 \times 1.8 \times 0.9$ m (length \times width \times height). Young adult dogs were food-restricted by missing one regular meal before the experiment to enhance motivation. To qualify for the test, food-restricted dogs needed to show interest in their favorite canned chicken (Xianyu, Wuhan, China) presented by the familiar experimenter at the test arena. WT dogs were interested in the food at the first time of the trial. However, it took a few trials (one trial/day) for some of the *bShank3* mutants to be familiar enough with the context to get the food. In the step 1 of the experiment, an individual dog freely explored the small cage containing a piece of sausage for 2 min in the absence of an experimenter. The dog could not open the cage containing food by himself. The experimenter then opened the cage and fed the dog with the sausage (step 2). In the test (step 3), the dog was allowed to explore the food-locked cage freely for 2 min, while the experimenter stood at the most distant side outside the puppy pen and looked at the cage with neutral expressions. The latency for the first gaze at the experimenter and the frequency of attention-seeking gaze in the first trial of the assay were statistically analyzed.

Machine learning-based analysis of tail wagging

Machine learning-based analysis of kinematic parameters such as frequency, amplitude and velocity of tail wagging during dog–human interactions was carried out as previously described [36].

Statistical analysis

The duration and frequency of a specific behavior including social interaction and social withdrawal were statistically analyzed manually by trained scorers who were blind to the genotype (each animal was coded for behavioral assays). We used one-way ANOVA to determine statistical significance among different groups. All tested samples/animals were included in the analysis. Sample size was not calculated a priori. Before analyzing the difference among different groups, we first analyzed the normality distribution of data by Graphpad Prism 8.0. One-way ANOVA was used in non-parameter manner for data with non-normality distribution or in parameter manner for data with normality distribution. Calculations were performed with GraphPad Prism 8.0 software. Data are presented as the mean \pm SD.

DATA AVAILABILITY

The raw whole-genome sequence data from founder mutants and WT parents are deposited in the Genome Sequence Archive in National Genomics Data Center, China National Center for Bioinformation, Chinese Academy of Sciences, under accession number CRA004090 and publicly accessible at <https://bigd.big.ac.cn/gsa>.

REFERENCES

1. De Rubeis S, He X, Goldberg AP, Poultnery CS, Samocha K, Cicek AE, et al. Synaptic, transcriptional and chromatin genes disrupted in autism. *Nature*. 2014;515:209–15.
2. Iossifov I, O'Roak BJ, Sanders SJ, Ronemus M, Krumm N, Levy D, et al. The contribution of de novo coding mutations to autism spectrum disorder. *Nature*. 2014;515:216–21.

3. Satterstrom FK, Kosmicki JA, Wang J, Breen MS, De Rubeis S, An JY, et al. Large-scale exome sequencing study implicates both developmental and functional changes in the neurobiology of autism. *Cell*. 2020;180:568–84.e523.
4. Fu JM, Satterstrom FK, Peng M, Brand H, Collins RL, Dong S, et al. Rare coding variation provides insight into the genetic architecture and phenotypic context of autism. *Nat Genet*. 2022;54:1320–31.
5. Zhou X, Feliciano P, Shu C, Wang T, Astrovskaia I, Hall JB, et al. Integrating de novo and inherited variants in 42,607 autism cases identifies mutations in new moderate-risk genes. *Nat Genet*. 2022;54:1305–19.
6. Jennings CG, Landman R, Zhou Y, Sharma J, Hyman J, Movshon JA, et al. Opportunities and challenges in modeling human brain disorders in transgenic primates. *Nat Neurosci*. 2016;19:1123–30.
7. Berry-Kravis EM, Lindemann L, Jonch AE, Apostol G, Bear MF, Carpenter RL, et al. Drug development for neurodevelopmental disorders: lessons learned from fragile X syndrome. *Nat Rev Drug Discov*. 2018;17:280–99.
8. Liu Z, Li X, Zhang JT, Cai YJ, Cheng TL, Cheng C, et al. Autism-like behaviours and germline transmission in transgenic monkeys overexpressing MeCP2. *Nature*. 2016;530:98–102.
9. Chen Y, Yu J, Niu Y, Qin D, Liu H, Li G, et al. Modeling Rett syndrome using TALEN-Edited MECP2 mutant cynomolgus monkeys. *Cell*. 2017;169:945–55.e910.
10. Zhao H, Tu Z, Xu H, Yan S, Yan H, Zheng Y, et al. Altered neurogenesis and disrupted expression of synaptic proteins in prefrontal cortex of SHANK3-deficient non-human primate. *Cell Res*. 2017;27:1293–7.
11. Tu Z, Zhao H, Li B, Yan S, Wang L, Tang Y, et al. CRISPR/Cas9-mediated disruption of SHANK3 in monkey leads to drug-treatable autism-like symptoms. *Hum Mol Genet*. 2019;28:561–71.
12. Zhou Y, Sharma J, Ke Q, Landman R, Yuan J, Chen H, et al. Atypical behaviour and connectivity in SHANK3-mutant macaques. *Nature*. 2019;570:326–31.
13. Zhao H, Jiang YH, Zhang YQ. Modeling autism in non-human primates: opportunities and challenges. *Autism Res*. 2018;11:686–94.
14. Feng G, Jensen FE, Greely HT, Okano H, Treue S, Roberts AC, et al. Opportunities and limitations of genetically modified nonhuman primate models for neuroscience research. *Proc Natl Acad Sci USA*. 2020;117:24022–31.
15. Lindblad-Toh K, Wade CM, Mikkelsen TS, Karlsson EK, Jaffe DB, Kamal M, et al. Genome sequence, comparative analysis and haplotype structure of the domestic dog. *Nature*. 2005;438:803–19.
16. Hong H, Zhao Z, Huang X, Guo C, Zhao H, Wang GD, et al. Comparative proteome and cis-regulatory element analysis reveals specific molecular pathways conserved in dog and human brains. *Mol Cell Proteom*. 2022;21:100261.
17. Hare B, Brown M, Williamson C, Tomasello M. The domestication of social cognition in dogs. *Science*. 2002;298:1634–6.
18. Miklosi A, Kubinyi E, Topal J, Gacsi M, Viranyi Z, Csanyi V. A simple reason for a big difference: wolves do not look back at humans, but dogs do. *Curr Biol*. 2003;13:763–6.
19. Teglas E, Gergely A, Kupan K, Miklosi A, Topal J. Dogs' gaze following is tuned to human communicative signals. *Curr Biol*. 2012;22:209–12.
20. Nagasawa M, Mitsui S, En S, Ohtani N, Ohta M, Sakuma Y, et al. Social evolution. Oxytocin-gaze positive loop and the coevolution of human-dog bonds. *Science*. 2015;348:333–6.
21. Jiang YH, Ehlers MD. Modeling autism by SHANK gene mutations in mice. *Neuron*. 2013;78:8–27.
22. Durand CM, Betancur C, Boeckers TM, Bockmann J, Chaste P, Fauchereau F, et al. Mutations in the gene encoding the synaptic scaffolding protein SHANK3 are associated with autism spectrum disorders. *Nat Genet*. 2007;39:25–7.
23. Wang X, McCoy PA, Rodriguez RM, Pan Y, Je HS, Roberts AC, et al. Synaptic dysfunction and abnormal behaviors in mice lacking major isoforms of Shank3. *Hum Mol Genet*. 2011;20:3093–108.
24. Wang X, Bey AL, Katz BM, Badea A, Kim N, David LK, et al. Altered mGluR5-Homer scaffolds and corticostriatal connectivity in a Shank3 complete knockout model of autism. *Nat Commun*. 2016;7:11459.
25. Anderson AC. Beagle as an experimental dog. Ames: Iowa University Press; 1970. p. 616.
26. Bolman B. Dogs for life: Beagles, drugs, and capital in the twentieth century. *J Hist Biol*. 2022;55:147–79.
27. Wang X, Xu Q, Bey AL, Lee Y, Jiang YH. Transcriptional and functional complexity of Shank3 provides a molecular framework to understand the phenotypic heterogeneity of SHANK3 causing autism and Shank3 mutant mice. *Mol Autism*. 2014;5:30.
28. Niu Y, Shen B, Cui Y, Chen Y, Wang J, Wang L, et al. Generation of gene-modified cynomolgus monkey via Cas9/RNA-mediated gene targeting in one-cell embryos. *Cell*. 2014;156:836–43.
29. Siwak CT, Tapp PD, Milgram NW. Effect of age and level of cognitive function on spontaneous and exploratory behaviors in the beagle dog. *Learn Mem*. 2001;8:317–25.
30. Moy SS, Nadler JJ, Perez A, Barbaro RP, Johns JM, Magnuson TR, et al. Sociability and preference for social novelty in five inbred strains: an approach to assess autistic-like behavior in mice. *Genes Brain Behav*. 2004;3:287–302.
31. Silverman JL, Yang M, Lord C, Crawley JN. Behavioural phenotyping assays for mouse models of autism. *Nat Rev Neurosci*. 2010;11:490–502.
32. Peca J, Feliciano C, Ting JT, Wang W, Wells MF, Venkatraman TN, et al. Shank3 mutant mice display autistic-like behaviours and striatal dysfunction. *Nature*. 2011;472:437–42.
33. Serpell J. The domestic dog: its evolution, behaviour and interactions with people. Cambridge: Cambridge University Press; 1995.
34. Quaranta A, Siniscalchi M, Vallortigara G. Asymmetric tail-wagging responses by dogs to different emotive stimuli. *Curr Biol*. 2007;17:R199–201.
35. Bradshaw J, Rooney N. Dog social behavior and communication. In: Serpell J, editor. The domestic dogs. Cambridge: Cambridge University Press; 2016. p. 133–59.
36. Ren W, Wei P, Yu S, Zhang YQ. Left-right asymmetry and attractor-like dynamics of dog's tail wagging during dog-human interactions. *iScience*. 2022;25:104747.
37. Siniscalchi M, d'Ingeo S, Minunno M, Quaranta A. Communication in dogs. *Animals*. 2018;8:131.
38. Muller CA, Schmitt K, Barber AL, Huber L. Dogs can discriminate emotional expressions of human faces. *Curr Biol*. 2015;25:601–5.
39. Hekman JP, Karas AZ, Sharp CR. Psychogenic stress in hospitalized dogs: cross species comparisons, implications for health care, and the challenges of evaluation. *Animals*. 2014;4:331–47.
40. Beerda B. Behavioral and hormonal indicators of enduring environmental stress in dogs. *Anim Welf*. 2000;2000:49–62.
41. Marshall-Pescini S, Colombo E, Passalacqua C, Merola I, Prato-Previde E. Gaze alternation in dogs and toddlers in an unsolvable task: evidence of an audience effect. *Anim Cogn*. 2013;16:933–43.
42. Soorya L, Kolevzon A, Zweifach J, Lim T, Dobry Y, Schwartz L, et al. Prospective investigation of autism and genotype-phenotype correlations in 22q13 deletion syndrome and SHANK3 deficiency. *Mol Autism*. 2013;4:18.
43. Leblond CS, Nava C, Polge A, Gauthier J, Huguet G, Lumbroso S, et al. Meta-analysis of SHANK Mutations in Autism Spectrum Disorders: a gradient of severity in cognitive impairments. *PLoS Genet*. 2014;10:e1004580.
44. De Rubeis S, Siper PM, Durkin A, Weissman J, Muratet F, Halpern D, et al. Delineation of the genetic and clinical spectrum of Phelan-McDermid syndrome caused by SHANK3 point mutations. *Mol Autism*. 2018;9:31.
45. Bozdagi O, Sakurai T, Papapetrou D, Wang X, Dickstein DL, Takahashi N, et al. Haploinsufficiency of the autism-associated Shank3 gene leads to deficits in synaptic function, social interaction, and social communication. *Mol Autism*. 2010;1:15.
46. Duffney LJ, Zhong P, Wei J, Matas E, Cheng J, Qin L, et al. Autism-like deficits in Shank3-deficient mice are rescued by targeting actin regulators. *Cell Rep*. 2015;11:1400–13.
47. Jaramillo TC, Speed HE, Xuan Z, Reimers JM, Liu S, Powell CM. Altered striatal synaptic function and abnormal behaviour in Shank3 exon4-9 deletion mouse model of autism. *Autism Res*. 2016;9:350–75.
48. Qin L, Ma K, Wang ZJ, Hu Z, Matas E, Wei J, et al. Social deficits in Shank3-deficient mouse models of autism are rescued by histone deacetylase (HDAC) inhibition. *Nat Neurosci*. 2018;21:564–75.
49. Dellling JP, Boeckers TM. Comparison of SHANK3 deficiency in animal models: phenotypes, treatment strategies, and translational implications. *J Neurodev Disord*. 2021;13:55.
50. Monteiro P, Feng G. SHANK proteins: roles at the synapse and in autism spectrum disorder. *Nat Rev Neurosci*. 2017;18:147–57.
51. Dawson G, Lewy A. Arousal, attention, and the socioemotional impairments of individuals with autism. In: Dawson G, editor. Autism: nature, diagnosis, and treatment. New York: Guilford Press; 1989. p. 49–74.
52. Weiss JA, Thomson K, Chan L. A systematic literature review of emotion regulation measurement in individuals with autism spectrum disorder. *Autism Res*. 2014;7:629–48.
53. Lai MC, Lombardo MV, Baron-Cohen S. Autism. *Lancet*. 2014;383:896–910.
54. Huang K, Han Y, Chen K, Pan H, Zhao G, Yi W, et al. A hierarchical 3D-motion learning framework for animal spontaneous behavior mapping. *Nat Commun*. 2021;12:2784.
55. Marshall JD, Aldarondo DE, Dunn TW, Wang WL, Berman GJ, Olveczky BP. Continuous whole-body 3d kinematic recordings across the rodent behavioral repertoire. *Neuron*. 2021;109:420–37.e428.
56. Ren W, Huang K, Li Y, Yang Q, Wang L, Guo K, et al. Altered pupil responses to social and non-social stimuli in Shank3 mutant dogs. *Mol Psychiatry*. Accepted.
57. Feng C, Wang X, Shi H, Yan Q, Zheng M, Li J, et al. Generation of ApoE deficient dogs via combination of embryo injection of CRISPR/Cas9 with somatic cell nuclear transfer. *J Genet Genom*. 2018;45:47–50.

58. Luo X, He Y, Zhang C, He X, Yan L, Li M, et al. Trio deep-sequencing does not reveal unexpected off-target and on-target mutations in Cas9-edited rhesus monkeys. *Nat Commun.* 2019;10:5525.
59. Li H, Handsaker B, Wysoker A, Fennell T, Ruan J, Homer N, et al. The sequence alignment/map format and SAMtools. *Bioinformatics.* 2009;25:2078–9.
60. Robinson JT, Thorvaldsdottir H, Winckler W, Guttman M, Lander ES, Getz G, et al. Integrative genomics viewer. *Nat Biotechnol.* 2011;29:24–6.

ACKNOWLEDGEMENTS

We thank Prof. X. Yu, X. Li, X. Xu, K. Guo, R. Zhang and A. Andics for discussion. This work was supported in part by the Ministry of Science and Technology of China (2019YFA0707100 and 2021ZD0203901), the National Natural Science Foundation of China (31830036, 31730039, and 31921002), the National Major Scientific Instruments and Equipment Development Project (ZDYZ2015-2), the Chinese Academy of Sciences Strategic Priority Research Program B grants (XDBS1020100, and XDB32010300), and Spring City Plan: the High-level Talent Promotion and Training Project of Kunming (2022SCP001).

AUTHOR CONTRIBUTIONS

YHJ and YQZ conceptualized the project, supervised data collection and analysis. XW and LL performed gene targeting. HL, YZ, and GW analyzed sequencing data. HX and HZ performed Western analysis. RT, HZ, YL, and QS designed and performed behavioral experiments. JZ, ZS, JM, WL, and WR assisted data collection and analysis. RT, HZ, LY and YQZ wrote the manuscript, and YHJ and YQZ finalized the manuscript.

COMPETING INTERESTS

The authors declare no competing interests.

ADDITIONAL INFORMATION

Supplementary information The online version contains supplementary material available at <https://doi.org/10.1038/s41380-023-02276-9>.

Correspondence and requests for materials should be addressed to Yong-hui Jiang or Yong Q. Zhang.

Reprints and permission information is available at <http://www.nature.com/reprints>

Publisher's note Springer Nature remains neutral with regard to jurisdictional claims in published maps and institutional affiliations.

Springer Nature or its licensor (e.g. a society or other partner) holds exclusive rights to this article under a publishing agreement with the author(s) or other rightsholder(s); author self-archiving of the accepted manuscript version of this article is solely governed by the terms of such publishing agreement and applicable law.